Original Article

MECHANISTIC ROLE OF THBS1-LOADED HEK293-DERIVED EXOSOMES IN SUPPRESSING ENDOMETRIAL CANCER: INVOLVEMENT OF TGF-B SIGNALING AND EXTRACELLULAR MATRIX DYNAMICS

Suying Zheng[1], Wenxu Li[2], Can Wang[3], Yang Zhang[3], Wanping Huang[4], Meng Su[3,*]

[1]Department of Gynecology, Cangnan Affiliated Hospital of Wenzhou Medical University, 325800 Wenzhou, Zhejiang, China
[2]Department of Radiation Oncology, Wenzhou Geriatric Hospital, 325000 Wenzhou, Zhejiang, China
[3]Department of Radiation Oncology, The First Affiliated Hospital of Wenzhou Medical University, 325000 Wenzhou, Zhejiang, China
[4]Zhejiang South Institute of Radiation Medicine and Nuclear Technology Application, 325809 Wenzhou, Zhejiang, China

Abstract

Background: Endometrial cancer (EC) is a prevalent gynecological malignancy with limited therapeutic options due to drug resistance and systemic toxicity. Exosomes have emerged as promising targeted drug delivery vehicles, but their application in EC remains underexplored. Thrombospondin-1 (THBS1), a key regulator of extracellular matrix remodeling and transforming growth factor β (TGF-β) signaling, may offer a novel therapeutic strategy for EC. **Methods:** Differentially expressed genes were identified from the public transcriptomic datasets and subjected to GO and KEGG enrichment analyses. Exosomes derived from Human embryonic kidney 293 (HEK293) cells overexpressing THBS1 were isolated and characterized by Western blotting, transmission electron microscopy, and nanoparticle tracking analysis. Their effects on EC cells were assessed using Cell Counting Kit-8, 5-ethynyl-2'-deoxyuridine incorporation, colony formation, wound healing, and cell invasion assays. TGF-β pathway involvement was assessed using the agonist SRI-011381. *In vivo* experiments were conducted to evaluate tumor growth, epithelial–mesenchymal transition (EMT) marker expression, and treatment safety. **Results:** THBS1 expression was downregulated in the EC cells. The restoration of THBS1 expression through exosome delivery inhibited cell proliferation, migration, and invasion. THBS1-overexpressing exosomes attenuated the activation of the TGF-β/Smad pathway and modulated EMT-related markers. The inhibitory effects of THBS1-exosomes were reversed by SRI-011381. *In vivo*, THBS1-exosome treatment markedly suppressed tumor growth, enhanced E-cadherin expression, reduced vimentin levels, and exhibited no observable toxicity. **Conclusions:** Exosomes overexpressing THBS1 effectively suppressed EC progression by targeting the TGF-β/Smad signaling axis and EMT. These findings support the potential of THBS1-enriched exosomes as a novel, safe, and targeted therapeutic modality for future EC.

Keywords: Endometrial cancer, thrombospondin-1, exosomes, TGF-β/Smad signaling, epithelial-mesenchymal transition.

***Address for correspondence**: Meng Su, Department of Radiation Oncology, The First Affiliated Hospital of Wenzhou Medical University, 325000 Wenzhou, Zhejiang, China. E-mail: smeng1989@163.com.

Introduction

Endometrial cancer (EC) is among the most prevalent gynecologic malignancies and substantially contributes to cancer-related morbidity and mortality in women worldwide [1]. Early-stage EC is often effectively managed through surgical resection, frequently supplemented with adjuvant radiotherapy or chemotherapy, but prolonged treatment regimens can impose considerable physical and psychological burdens on patients [2,3]. Despite advancements in molecular profiling and targeted therapies [4, 5], the clinical efficacy of these approaches remains constrained by challenges, such as drug resistance, systemic toxicity, and suboptimal response rates. These limitations highlight the urgent need to identify novel therapeutic strategies that offer both improved efficacy and tolerability.

Exosomes have garnered considerable attention as versatile platforms for cancer diagnostics and treatment [6–8]. These small extracellular vesicles, typically ranging from 50 to 400 nm in size, are released by a wide variety of biological fluids [9]. They facilitate cell-to-cell signaling through the transfer of cell types and are detectable in numerous biological fluids. Functioning as mediators of intercellular communication, exosomes transport a diverse

array of bioactive molecules, including proteins, lipids, and nucleic acid molecules [10]. Increasing evidence has implicated exosomes in the regulation of key tumor-related processes, such as cell proliferation, metastasis, immune evasion, and resistance [11–13]. Their intrinsic properties, namely, high biocompatibility, stability in circulation, and ability to cross physiological barriers, render exosomes particularly attractive for clinical applications in disease monitoring and targeted treatment [14–16]. Notably, bioengineered exosomes can be precisely modified to deliver therapeutic agents or disrupt oncogenic signaling pathways. These features underscore their potential as a flexible and safe modality in the context of cancer therapy [17–19].

Among the molecular pathways implicated in the progression of EC, the transforming growth factor-β (TGF-β) signaling cascade has attracted considerable attention [20,21]. Specifically, the TGF-β/Smad axis plays a pivotal role in regulating epithelial-mesenchymal transition (EMT)—a dynamic cellular program through which epithelial cells lose their polarity and intercellular adhesion, acquiring mesenchymal [22]. This phenotypic transformation is critically involved in tumor invasion, metastasis and the development of resistance to therapy. The dysregulation of TGF-β signaling and aberrant activation of EMT signaling have been widely observed in various malignancies, including EC [23,24]. Therefore, therapeutic strategies targeting the TGF-β/Smad axis and EMT-related mechanisms offer considerable promise for mitigating cancer progression.

In this study, we conducted comprehensive bioinformatics analyses using The Cancer Genome Atlas Uterine Corpus Endometrial Carcinoma (TCGA-UCEC) dataset to identify differentially expressed genes (DEGs) contributing to EC pathogenesis. Functional enrichment analyses revealed that the TGF-β signaling and extracellular matrix (ECM)–receptor interaction pathways played a substantial role in EC progression. Based on these findings, we selected to examine thrombospondin-1 (*THBS1*), which is a key gene enriched in both pathways. Then, we subsequently explored the application of exosomes produced by human embryonic kidney 293 (HEK293) cells to assess their influence on tumor-related behaviors in EC cell lines. Furthermore, we examined the extent to which these effects are mediated through the TGF-β/Smad cascade and EMT regulation. Our findings provide novel mechanistic insights into the tumor-suppressive role of THBS1-enriched exosomes in EC and underscore their potential as a novel therapeutic platform for advancing exosome-based treatments in gynecological oncology.

Methods

Bioinformatics Analysis

Gene expression profiles and corresponding clinical data of endometrial cancer patients with EC were obtained from the TCGA-UCEC dataset. DEGs were identified using the "limma" package in R (Version 4.1.2; R Foundation for Statistical Computing, Vienna, Austria) with filtering criteria set at |log2 fold change (FC)| $>$ 2 and adjusted p-value $<$ 0.05. A volcano plot was generated to illustrate the global gene expression landscape. Weighted gene co-expression network analysis (WGCNA) was performed using the "WGCNA" R package. The top 5000 genes, ranked by absolute median deviation, were selected for network construction. An optimal soft-thresholding parameter was determined using the "pickSoftThreshold" function, and the assessed candidate powers ranged from 1 to 20. A power value of 12 was ultimately selected for subsequent module detection. On the basis of this threshold, four distinct gene modules were identified. The topological overlap matrix and the resulting hierarchical clustering dendrogram were utilized to visualize the gene interconnectivity, which was represented as a heatmap. To identify key regulatory genes, a Venn diagram was employed to assess the intersection between the DEGs and genes within the most relevant WGCNA module. Genes present in both datasets were considered candidate key genes for further investigation. Protein–protein interaction (PPI) networks of these overlapping genes were constructed using the STRING database (https://string-db.org/) and visualized using Cytoscape (Version 3.10.2; Institute for Systems Biology, Seattle, WA, USA). Functional annotation and pathway enrichment analyses of the candidate genes were conducted using GO and KEGG analyses via the "clusterProfiler" R package, providing comprehensive insights into their functional roles.

Cell Culture and Transfection

Human endometrial stromal cells (ESCs; Procell, Wuhan, China, CP-H208) were cultured in Dulbecco's modified Eagle's medium (DMEM)/nutrient mixture F-12 (Solarbio, Beijing, China, D6501) supplemented with 10% fetal bovine serum (FBS; Solarbio, Beijing, China, S9020) and 1% penicillin–streptomycin solution (Beyotime, Shanghai, China, C0222). HEK293 cells (Procell, Wuhan, China, CP-H208), along with human EC cell lines, including Ishikawa (Ish; CL-0283), KLE (CL-0133), and RL95-2 (CL-0197), were obtained from Procell (Wuhan, China) and maintained in complete DMEM supplemented with 10% FBS and 1% penicillin–streptomycin solution. All cell lines were cultured in a humidified incubator at 37 °C with 5% CO_2. Prior to experimentation, all cell lines were authenticated through short tandem repeat profiling and confirmed to be free of mycoplasma contamination. To pharmacologically activate TGF-β signaling, we treated the cells with 10 μM of the small-molecule agonist SRI-011381 (MedChemExpress, NJ, USA, HY-120620) [25].

For the generation of stable THBS1-overexpressing cell lines, lentiviral particles were produced by inserting the full-length human *THBS1* coding sequence (NM_003246.3) into the pLV-EF1α-MCS-IRES-Puro backbone vector (GeneChem, Shanghai, China). Cells were transduced with lentiviral particlesen coding either

Table 1. Primer sequences.

Primer	Sequences (5'-3')	Expected amplicon lengths
THBS1	F: GCTGGAAATGTGGTGCTTGTCC R: CTCCATTGTGGTTGAAGCAGGC	108 bp
E-cadherin	F: GGTCATCAGTGTGCTCACCTCT R: GCTGTTGTGCTCAAGCCTTCAC	105 bp
Vimentin	F: CGGAAAGTGGAATCCTTGCAGG R: AGCAGTGAGGTCAGGCTTGGAA	138 bp
GAPDH	F: GTCTCCTCTGACTTCAACAGCG R: ACCACCCTGTTGCTGTAGCCAA	131 bp

the *THBS1* sequence or the empty control vector at a multiplicity of infection (MOI) of 10 in the presence of 8 μg/mL polybrene (Sigma-Aldrich, MO, USA, TR-1003). After a 48-h incubation period, transduced cells were subjected to selection with 2.5 μg/mL puromycin. Surviving cells were subsequently expanded and validated for stable THBS1 overexpression via Western blotting and quantitative real-time PCR. The same procedure was employed to generate THBS1-overexpressing HEK293 cells.

Quantitative Real-Time PCR (RT-qPCR)

Total cellular RNA was extracted using TRIzol reagent (Sigma-Aldrich, St. Louis, MO, USA; T9424) following the manufacturer's protocol. Subsequently, 1 μg of RNA was reverse-transcribed into complementary DNA using a PrimeScript^{TM} RT reagent kit with gDNA eraser (Takara, Shiga, Japan, RR047A). RT-qPCR was performed using SYBR Green Master Mix (Applied Biosystems, Foster City, CA, USA, 4367659) on a QuantStudio 3 real-Time PCR System (Applied Biosystems, USA, A28137). We examined *GAPDH* expression levels in exosomal RNA preparations. *GAPDH* was consistently detected and its Ct value was stable across independent HEK293-derived exosome samples. *GAPDH* was used as the internal reference gene, and relative mRNA expression levels were calculated using the 2^{-Ct} method. The primer sequences used in this study are listed in Table 1.

Western Blot Analysis

Proteins from cells and exosomes were extracted using RIPA lysis buffer (Beyotime, Shanghai, China, P0013B), and quantified using a BCA protein assay kit (Thermo Fisher Scientific, Waltham, MA, USA, 23227). Equal amounts of protein were separated through SDS-PAGE, and transferred to PVDF membranes. Following blocking with 5% nonfat milk, the membranes were incubated overnight at 4 °C with the following primary antibodies: anti-THBS1 (Proteintech, Wuhan, China, 18304-1-AP, 1:1000), anti-TGF-β (Abcam, Cambridge, UK, ab215715, 1:1000), anti-p-Smad2 (Abcam, Cambridge, UK, ab280888, 1:1000), anti-Smad2 (Abcam, Cambridge, UK, ab40855, 1:2000), anti-p-Smad3 (Abcam, Cambridge, UK, ab52903, 1:2000), anti-Smad3 (Abcam, Cambridge, UK, ab40854, 1:1000), anti-E-cadherin (Abcam, Cambridge, UK, ab40772, 1:1000), anti-vimentin (Abcam, Cambridge, UK, ab92547, 1:1000), anti-CD9 (Abcam, Cambridge, UK, ab236630, 1:1000), anti-CD63 (Abcam, Cambridge, UK, ab134045, 1:1000), anti-CD81 (Abcam, Cambridge, UK, ab79559, 1:1000), anti-TSG101 (Abcam, Cambridge, UK, ab125011, 1:1000), and anti-GAPDH (Abcam, Cambridge, UK, ab8254, 1:1000). After washing, the membranes were incubated for 1 h at ambient temperature with horseradish peroxidase-conjugated secondary antibodies (goat anti-mouse IgG, ab97040; or goat anti-rabbit IgG, ab288151, Abcam, Cambridge, UK). Protein bands were visualized using an enhanced chemiluminescence (ECL) detection reagent (Bio-Rad, California, USA, 1705061) and imaged using a ChemiDoc imaging system (Bio-Rad, CA, USA, 12003154).

Cell Viability and Proliferation Assays

Cell viability was assessed using the Cell Counting Kit-8 (CCK-8; Beyotime, Shanghai, China, C0037) according to the manufacturer's instructions. Cells were seeded into a 96-well plate and assessed at 0, 24, 48, and 72 h. At each time point, CCK-8 reagent was added to the wells and incubated for 2 h at 37 °C. Absorbance was then measured at 450 nm with a microplate reader (BioTek, Winooski, VT, USA).

To assess cell proliferation, we performed a 5-ethynyl-2'-deoxyuridine (EdU) incorporation assay with a commercial kit (Beyotime, Shanghai, China, C0071S) in accordance with the manufacturer's protocol. Cells were seeded at a density of 1×10^5 cells per well and incubated with 10 μM EdU. Following incubation, the cells were fixed, permeabilized, and stained as instructed by the kit. Nuclei were counterstained with 5 μg/mL Hoechst 33342 (Beyotime, Shanghai, China, C1022). Fluorescent images were acquired using a fluorescence microscope (Leica, Wetzlar, Germany, DMi8) and analyzed with ImageJ software (National Institutes of Health, Bethesda, MD, USA, version 1.53t).

For the colony formation assays, the cells were seeded in 6-well plates at a density of 500–1000 cells per well and

cultured for two weeks. The colonies were then fixed with 4% paraformaldehyde, stained with 0.1% crystal violet solution (Beyotime, Shanghai, China, C0121), and washed with phosphate-buffered saline (PBS; Solarbio, Beijing, China, P1010). Colonies containing more than 50 cells were counted using ImageJ.

Migration and Invasion Assays

Cell migration ability was assessed through wound closure assays were performed to assess cell migratory ability. Cells grown to confluence, which were scratched with a pipette tip, washed with PBS, and cultured in a serum-free medium. Images at 0 and 24 h were captured, and wound closure was quantified using ImageJ to assess cell migration.

Transwell invasion assays were performed using Matrigel-coated 8.0 μm pore chambers (Corning, New York, NY, USA, 3422). Cells (1×10^5) in the serum-free medium were seeded in the upper chamber, and the lower chamber contained a 10% FBS medium. After 48 h, invaded cells were fixed, stained with crystal violet, imaged, and counted in five random fields.

Isolation and Characterization of HEK293-Derived Exosomes

Exosomes were isolated from THBS1-overexpressing HEK293 cell media through sequential centrifugation and ultracentrifugation at 100,000 × g. Pellets were washed, resuspended in PBS, and characterized by transmission electron microscopy (TEM; Hitachi, Tokyo, Japan, HT7700), nanoparticle tracking analysis (NTA; Particle Metrix, Meerbusch, Germany, ZetaView PMX120), and Western blotting for markers (CD9, CD63, CD81, TSG101). THBS1 expression was confirmed by RT-qPCR and Western blot.

Functional Assays of Exosome-Treated Cells

EC cells were treated with HEK293-derived exosomes either with or without *THBS1* overexpression at a concentration of 100 μg/mL for 48 h. To evaluate the functional impact of these exosomes on tumor cell behavior, a series of assays, including CCK-8, EdU incorporation, colony formation, wound closure, and Transwell invasion assays were performed as previously described. These experiments were designed to assess the modulatory effects of THBS1-enriched exosomes on cell viability, motility, and invasive potential.

In Vivo Tumor Xenograft Model

Four-week-old female BALB/c nude mice (n = 18, 18–20 g; SPF Biotechnology, Beijing, China) were housed under sterile, pathogen-free conditions. Approximately 1×10^6 logarithmically growing Ish cells suspended in 100 μL of PBS were subcutaneously injected into the left hind limb of each mouse. Once tumor volumes reached approximately 75 mm^3, the mice were randomly assigned to three groups (n = 6 per group): Control (received 100 μL of PBS via the tail vein), exo-ov-NC (received HEK293-derived exosomes transduced with empty vector), and exo-ov-THBS1 (received HEK293-derived exosomes overexpressing *THBS1*). Randomization was performed using a computer-generated random number sequence. The group size (n = 6) was determined based on a previous study [26]. Inclusion criteria were defined a priori and consisted of (1) healthy physical appearance upon arrival, and (2) successful tumor formation (palpable tumor $\geq$75 mm^3) prior to group allocation. No exclusion criteria were applied during the course of the study. The mice received tail vein injection of exosomes at a dosage of 6 mg/kg every other day for a total of 14 days. Tumor length (L) and width (W) were measured every other day using a vernier caliper (Meinaite, Guangdong, China, MN200), and tumor volume was calculated using the formula: volume = $(L \times W^2)/2$. Body weight was also monitored regularly as an indicator of systemic toxicity.

Primary outcome measures assessed included tumor volume as a quantitative indicator of therapeutic efficacy. Secondary outcomes included body weight changes, histopathological analysis of tumor tissues via H&E staining; and mRNA expression levels of *THBS1* and EMT-related markers (E-cadherin, N-cadherin, and vimentin) as determined by RT-qPCR. All 18 mice successfully developed tumors and completed the full treatment regimen without attrition. No animals or data points were excluded from the analysis. To minimize potential confounding variables, we housed all the mice under identical environmental conditions. Treatment administration and tumor and body weight measurements were performed at the same time of day by the same investigator, who adhered to a standardized schedule. Cage positions were rotated every three days to mitigate location-related bias. While the investigator responsible for group allocation was not blinded, all personnel involved in treatment administration, tumor measurements, histological evaluation, and data analysis were blinded to group assignments to reduce bias. At the end of the 14-day treatment period, all animals were humanely euthanized through intraperitoneal injection of sodium pentobarbital (100 mg/kg) followed by cervical dislocation, in accordance with institutional animal care and use guidelines. Tumors and major organs (liver and kidney) were harvested for further analysis. Tumor tissues were divided for downstream applications: One portion was fixed in 4% paraformaldehyde, paraffin-embedded, and subjected to H&E staining (Solarbio, Beijing, China, G1120) for histopathological assessment. The remaining tissue was used for RNA extraction and RT-qPCR analysis of *THBS1* and EMT-associated gene expression.

Statistical analysis

All experiments were performed in triplicate and independently repeated at least three times. Data are presented

as mean ± standard deviation (SD). Statistical analyses were conducted using GraphPad Prism software (GraphPad Software Inc., San Diego, CA, USA, version 9.0.5). Comparisons between two groups were performed using an unpaired, two-tailed Student's *t*-test. For comparisons involving three or more groups, one-way analysis of variance followed by Tukey's post hoc test was applied. Prior to conducting parametric analyses, data normality was evaluated using the Shapiro–Wilk test, and homogeneity of variances was assessed using Levene's test. When assumptions for parametric tests were not met, appropriate nonparametric alternatives, such as the Mann–Whitney U test or Kruskal–Wallis test were employed. A p-value of < 0.05 was considered statistically significant.

Results

Identification of key genes in endometrial cancer

To identify potential key genes potentially involved in EC pathogenesis, we performed differential gene analysis using the TCGA-UCEC dataset. This analysis identified 3786 DEGs according to the criteria FC > 2 and adjusted $p < 0.05$ (Fig. 1**a**). Subsequently, WGCNA was conducted using the top 5000 genes ranked by absolute median deviation, resulting in the construction of a hierarchical gene clustering dendrogram (Fig. 1**b**). Among the generated modules, the brown module demonstrated the strongest positive correlation with EC status (correlation coefficient = 0.73, $p < 0.01$; Fig. 1**c**). By intersecting the DEGs with genes within the brown module, a total of 76 overlapping candidates were identified (Fig. 1**d**). PPI network analysis of these overlapping genes revealed several hub genes with high connectivity (Fig. 1**e**). GO and KEGG enrichment analyses further demonstrated significant enrichment in biological processes and pathways associated with ECM organization, cell adhesion, and notably, the TGF-β signaling pathway and ECM–receptor interaction axis, both of which are critically implicated in tumor progression and EMT (Fig. 1**f** and **g**). Notably, *THBS1* was commonly enriched in both pivotal pathways and thus selected for subsequent functional and mechanistic analyses.

THBS1 expression and its effects on endometrial cancer cell behavior

To further elucidate the functional role of *THBS1* in EC, we examined its expression in normal human ESCs and EC cell lines, including Ish, KLE, and RL95-2. *THBS1* expression was markedly downregulated in all cancer cell lines compared with ESCs (Fig. 2**a**). To explore the biological effects of *THBS1*, we performed lentiviral-mediated overexpression in Ish and KLE cells. Successful overexpression was confirmed by Western blot and RT-qPCR (Fig. 2**b**–**d**). Functional assays revealed that *THBS1* overexpression significantly impaired the proliferative capacity of the EC cells. CCK-8 assays demonstrated reduced viability in THBS1-overexpressing Ish and KLE cells (Fig. 2**e** and **f**). Similarly, EdU incorporation assays showed a marked decrease in proliferating cells upon *THBS1* overexpression (Fig. 2**g** and **h**). In addition, colony formation assays indicated a reduction in the number of colonies formed by THBS1-overexpressing cells (Fig. 2**i** and **j**). To investigate the influence of *THBS1* on cell motility and invasiveness, we conducted wound healing and Transwell invasion assays. Wound closure assays revealed delayed scratch closure in THBS1-overexpressing cells, suggesting impaired migratory capacity (Fig. 3**a** and **b**). The number of cells traversing Matrigel-coated Transwell membranes was considerably reduced after *THBS1* overexpression, indicating suppressed invasive potential (Fig. 3**c** and **d**). Collectively, these results suggest that *THBS1* acts as a suppressor of cell proliferation, migration, and invasion in EC.

Effects of THBS1-overexpressing exosomes on endometrial cancer cells

Protein and mRNA analyses confirmed robust upregulation of *THBS1* in HEK293 cells transduced with THBS1-overexpressing lentiviral vectors, as validated by Western blot and RT-qPCR (Fig. 4**a**–**c**). Exosomes were then isolated from the conditioned medium of THBS1-overexpressing HEK293 cells and characterized by TEM and NTA. TEM imaging revealed the characteristic cup-shaped morphology of exosomes, and NTA indicated an average particle diameter of approximately 167 nm. (Fig. 4**d** and **e**). Western blot analysis further confirmed the presence of canonical exosomal surface markers, including CD9, CD81, CD63, and TSG101, validating successful isolation (Fig. 4**f**). Moreover, elevated levels of *THBS1* within the exosomes were confirmed by both Western blot and RT-qPCR (Fig. 4**g** and **h**). Functional assays demonstrated that treatment with THBS1–HEK293-derived exosomes suppressed the viability of Ish and KLE cells, as determined by the CCK-8 assays (Fig. 4**i** and **j**). Consistently, EdU incorporation and colony formation assays showed that THBS1–exosome treatment markedly impaired the proliferative capacity of both cell lines (Fig. 4**k**–**n**). In addition to their anti-proliferative effects, these exosomes exhibited inhibitory effects on cancer cell motility and invasiveness. Wound healing assays revealed delayed scratch closure in exosome-treated cells relative to controls, indicating reduced migratory activity (Fig. 5**a** and **b**). Similarly, Transwell invasion assays showed a significant reduction in the number of invading cells upon treatment with THBS1–HEK293-derived exosomes (Fig. 5**c** and **d**). Collectively, these findings indicate that THBS1-enriched exosomes exert potent antitumor effects *in vitro* by attenuating the proliferation, migration, and invasion of EC cells.

THBS1-exosome-mediated regulation of TGF-β/Smad signaling and EMT

To elucidate the underlying mechanism by which THBS1-enriched exosomes exert their effects on EC cells,

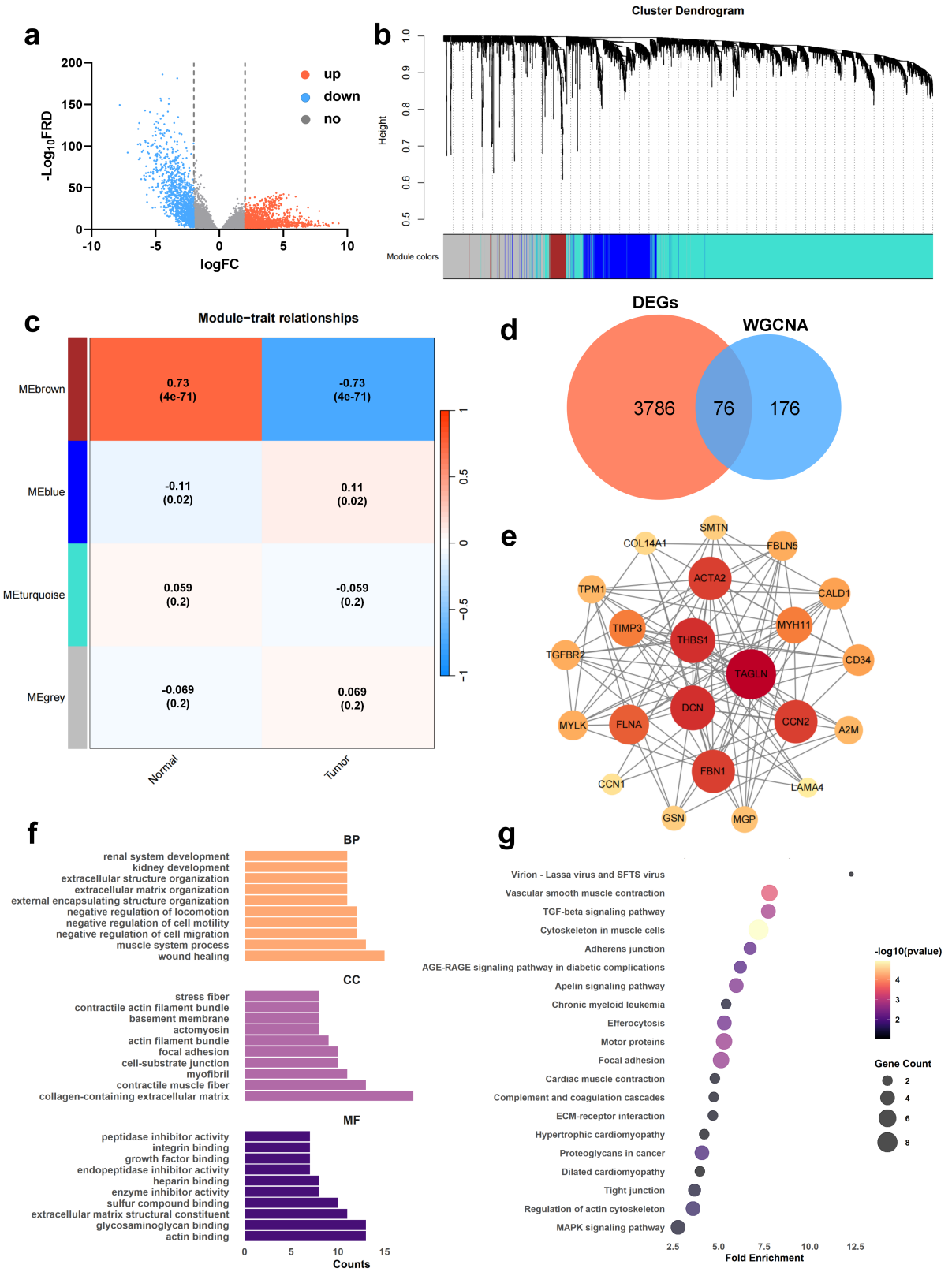

Fig. 1. Identification of key genes associated with endometrial cancer through integrated bioinformatics analysis. (**a**) DEGs based on the TCGA-UCEC dataset; (**b**) Gene clustering dendrogram of the top 5000 genes ranked by absolute median deviation in the UCEC samples (drawn with R 4.5.1); (**c**) Correlation between gene modules and disease traits (drawn with R 4.5.1); (**d**) Venn diagram showing intersecting genes between DEGs and the brown module (created with Microsoft PowerPoint); (**e**) PPI network of the intersecting genes (drawn with Cytoscape); (**f**) GO enrichment analysis of the intersecting genes (drawn with R 4.5.1); (**g**) KEGG pathway enrichment analysis of the intersecting genes (drawn with R 4.5.1).

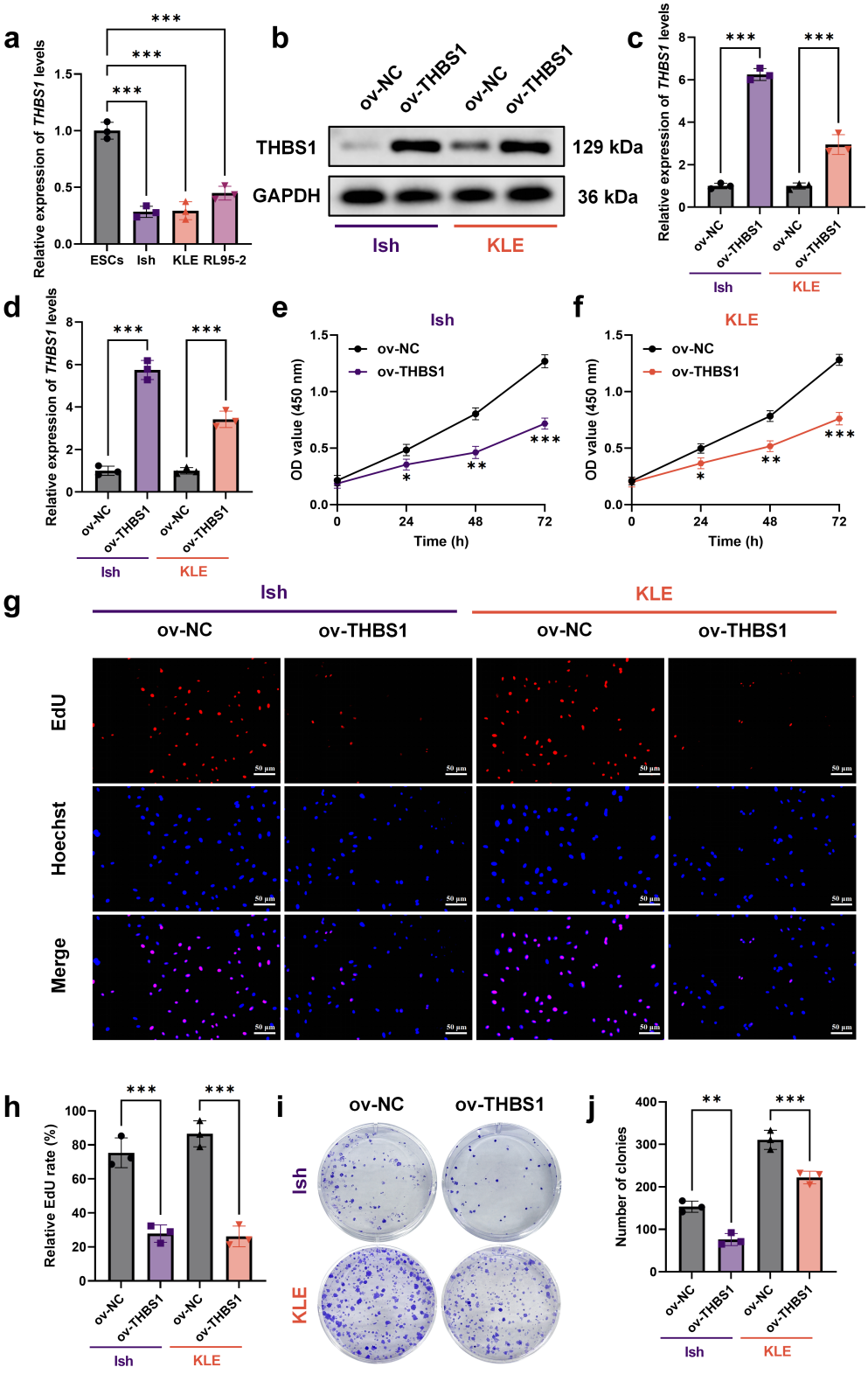

Fig. 2. THBS1 is downregulated in endometrial cancer cells and inhibits cell proliferation upon overexpression. (**a**) Expression levels of THBS1 in normal ESCs and endometrial cancer cell lines (Ish, KLE, RL95-2); (**b**, **c**) Western blot analysis confirming THBS1 overexpression efficiency in Ish and KLE cells after transfection; (**d**) RT-qPCR analysis of THBS1 mRNA levels following transfection; (**e**, **f**) CCK-8 assay showing decreased cell viability after THBS1 overexpression in Ish and KLE cells; (**g**, **h**) EdU assay demonstrating reduced cell proliferation (Scale bar: 50 μm); (**i**, **j**) Colony formation assay confirming the inhibitory effect of THBS1 overexpression on endometrial cancer cell growth. *$p < 0.05$, **$p < 0.01$, ***$p < 0.001$.

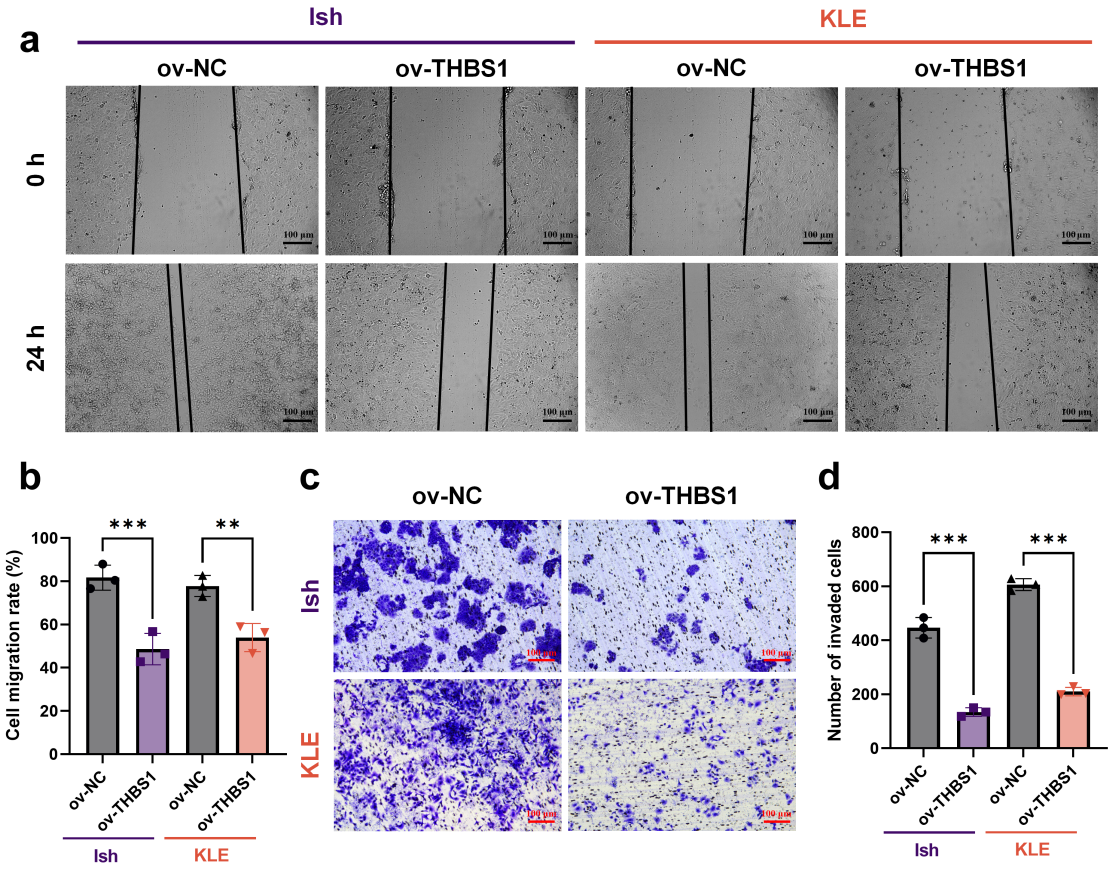

Fig. 3. *THBS1* overexpression suppresses migration and invasion of endometrial cancer cells. (**a**, **b**) Wound closure assay assessing the migratory capacity of Ish and KLE cells after *THBS1* overexpression (Scale bar: 100 μm); (**c**, **d**) Transwell invasion assay evaluating the invasive ability of THBS1-overexpressing Ish and KLE cells (Scale bar: 100 μm). $^{**}p < 0.01$, $^{***}p < 0.001$.

we focused on the TGF-β/Smad signaling pathway, a well-established regulator of tumor progression and EMT. Western blot analysis revealed that treatment with THBS1-overexpressing HEK293-derived exosomes considerably reduced the expression levels of phosphorylated Smad2 (p-Smad2), phosphorylated Smad3 (p-Smad3), and TGF-β in both Ish and KLE cells, while total Smad2 and Smad3 levels remained unchanged (Fig. 6**a**–**h**). Notably, inhibitory effects on pathway activation were effectively reversed upon co-treatment with SRI-011381, which is a small-molecule TGF-β activator, thereby confirming the functional involvement of the TGF-β/Smad axis in mediating the antitumor effects of THBS1-enriched exosomes.

Furthermore, treatment with THBS1-enriched exosomes led to a considerable downregulation of the mesenchymal marker vimentin and an upregulation of the epithelial marker E-cadherin, consistent with the suppression of EMT (Fig. 6**i**–**k**). These EMT-related changes were effectively reversed upon co-treatment with SRI-011381, further supporting the notion that THBS1-exosomes modulate EMT by inhibition of TGF-β signaling.

Effects of TGF-β pathway activation on THBS1-exosome-mediated inhibition of tumor cell behavior

To determine whether the tumor-suppressive effects of THBS1-enriched exosomes are mechanistically mediated through the inhibition of the TGF-β signaling, we evaluated EC cell phenotypes after co-treatment with SRI-011381. EdU incorporation and colony formation assays demonstrated that SRI-011381 reversed the antiproliferative effects induced by THBS1-exosomes in both Ish and KLE cell lines (Fig. 7**a**–**d**). Similarly, wound healing and Transwell invasion assays revealed that the inhibitory effects of THBS1-exosomes on cellular migration and invasiveness were notably mitigated by SRI-011381 (Fig. 7**e**–**h**). Collectively, these findings confirm that the antitumor activities of THBS1-exosomes are at least partially attributable to the suppression of the TGF-β signaling pathway.

In vivo effects of THBS1-exosomes on tumor growth and EMT marker expression

To further evaluate the therapeutic potential of THBS1-overexpressing exosomes, we established an EC xenograft model. As illustrated in the schematic diagram

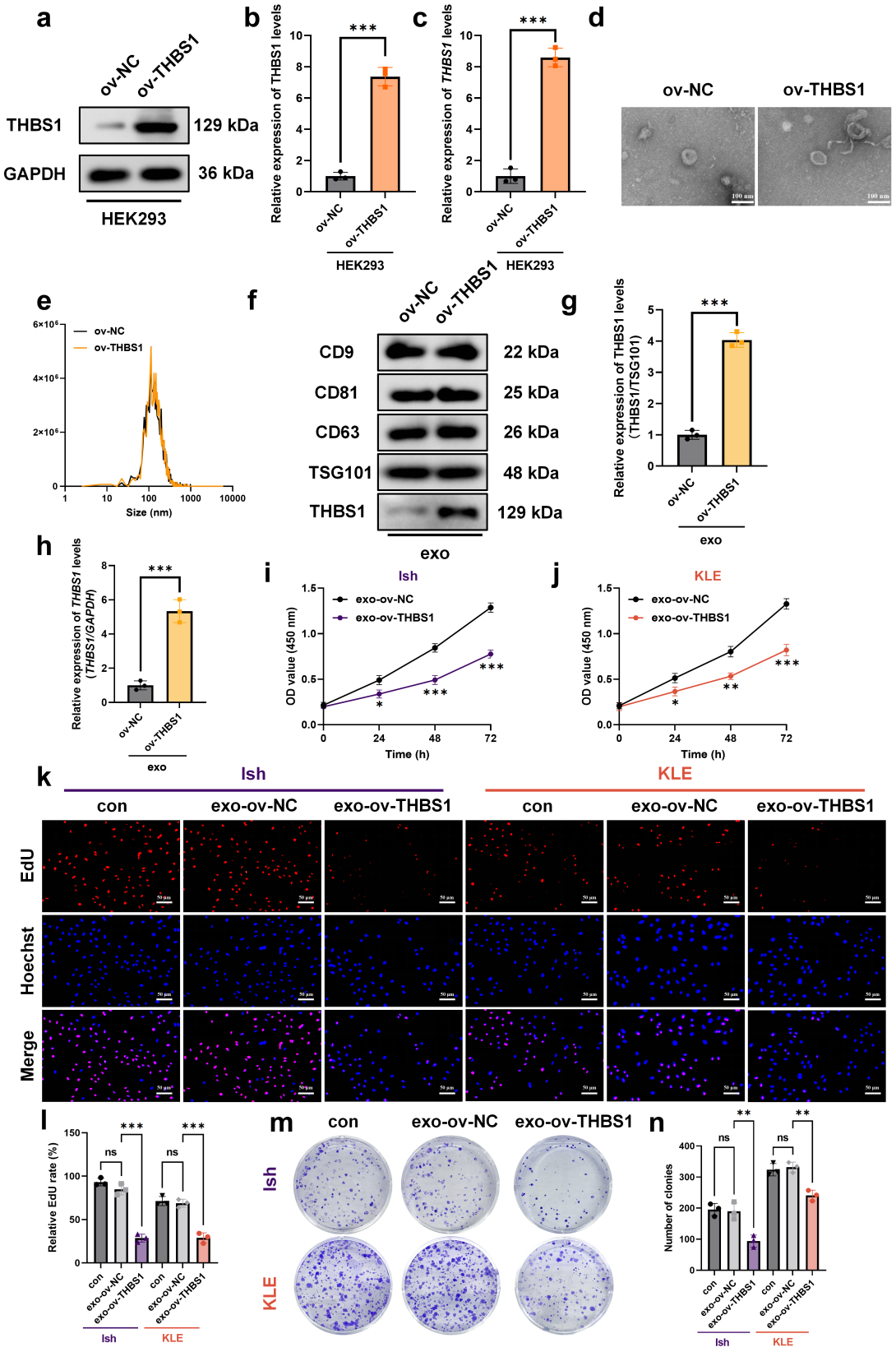

Fig. 4. Characterization of THBS1-overexpressing HEK293-derived exosomes and their inhibitory effects on endometrial cancer cell proliferation. (**a**, **b**) Western blot and (**c**) RT-qPCR analyses of *THBS1* expression in HEK293 cells stably overexpressing THBS1. (**d**) TEM imaging (Scale bar: 100 nm) and (**e**) NTA showing the morphology and size distribution of exosomes derived from THBS1-overexpressing HEK293. (**f**, **g**) Western blot analysis of exosomal markers (CD9, CD81, CD63, TSG101) and THBS1 protein expression in HEK293-derived exosomes. (**h**) RT-qPCR detection of *THBS1* expression in HEK293-derived exosomes. (**i**, **j**) CCK-8 assay assessing the viability of Ish and KLE cells treated with THBS1–HEK293-derived exosomes. (**k**, **l**) EdU assay (Scale bar: 50 μm) and (**m**, **n**) colony formation assay evaluating the proliferative capacity of endometrial cancer cells after treatment with THBS1–HEK293-derived exosomes. ns, not significant ($p > 0.05$), *$p < 0.05$, **$p < 0.01$, ***$p < 0.001$.

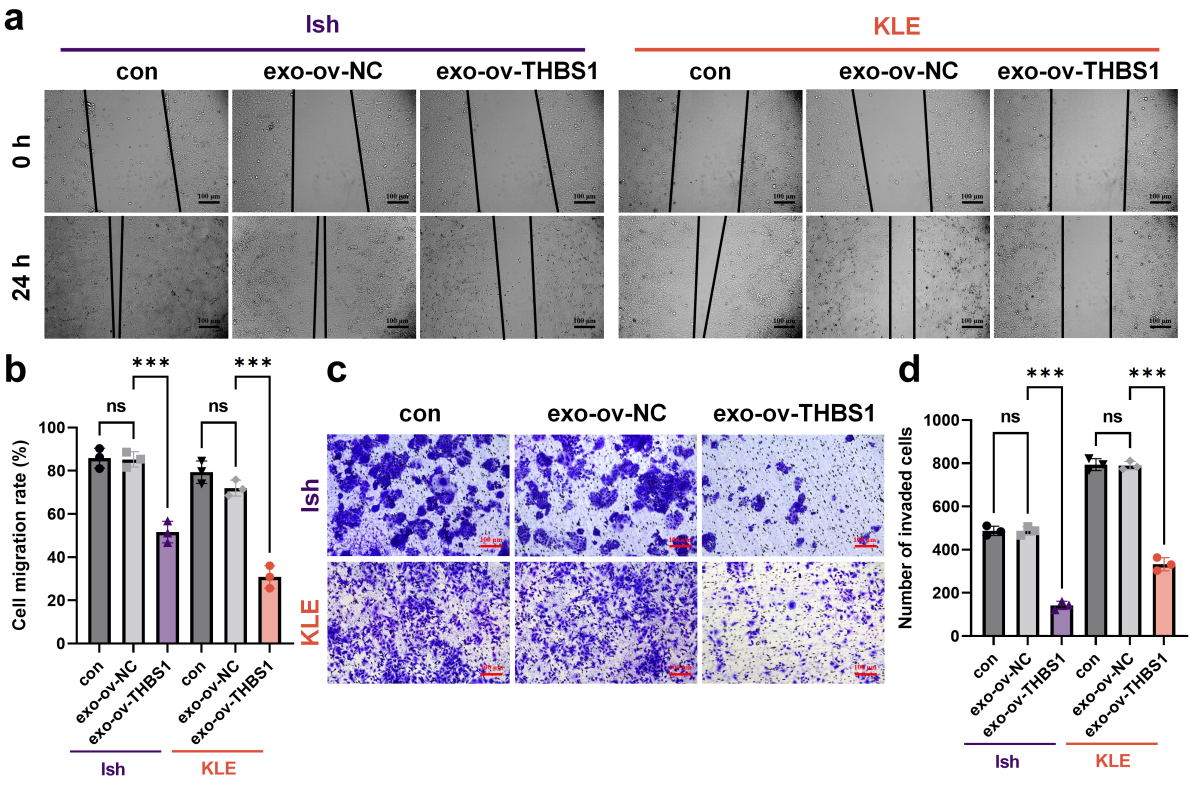

Fig. 5. THBS1-HEK293-derived exosomes suppress the migration and invasion of endometrial cancer cells. (**a**, **b**) Wound closure assay evaluating the migratory ability of Ish and KLE cells treated with THBS1-overexpressing HEK293-derived exosomes (Scale bar: 100 μm). (**c**, **d**) Transwell invasion assay assessing the invasive capacity of Ish and KLE cells following treatment with THBS1–HEK293-derived exosomes (Scale bar: 100 μm). ns, not significant ($p > 0.05$), ***$p < 0.001$.

(Fig. 8**a**), the mice received systemic administration of HEK293-derived exosomes. Tumor growth curves demonstrated that treatment with exo-ov-THBS1 inhibited tumor progression (Fig. 8**b**). This finding was corroborated by the markedly reduced tumor volumes at the study endpoint (Fig. 8**c**). Notably, body weight remained consistent across all groups throughout the treatment period, indicating no apparent systemic toxicity associated with exosome administration (Fig. 8**d**).

Additionally, H&E staining of major organs, including the liver, and kidney revealed no apparent histopathological abnormalities, further supporting the biosafety profile of the exosome-based treatment (Fig. 8**e**). RT-qPCR analysis of tumor tissues confirmed increased expression revealed upregulation of *THBS1* and the epithelial marker *E-cadherin*, alongside decreased expression of the mesenchymal marker vimentin, suggesting inhibition of EMT *in vivo* (Fig. 8**f**).

Discussion

Over the past decades, intensive research has aimed to develop more innovative and effective therapeutic strategies for EC [27,28]. Increasing evidence highlights the pivotal roles of the TGF-β signaling pathway and EMT in promoting malignant progression, metastasis, and therapeutic resistance across various cancers, including EC [29–31]. The dysregulation of these signaling cascades is known to augment tumor cell invasiveness and aggressiveness. In this study, we utilized transcriptomic data from the TCGA-UCEC dataset to perform differential gene expression analysis and WGCNA, allowing for the identification of gene modules highly associated with EC. Functional enrichment analyses of these gene sets revealed their crucial role in ECM remodeling, cell–cell adhesion, and TGF-β–related pathways—core biological processes fundamentally implicated in tumor progression. Notably, *THBS1* emerged as a key intersecting gene in the TGF-β signaling cascade and ECM–receptor interaction pathways, exhibiting a potential role as a central regulatory factor in EC pathogenesis.

THBS1 is a matricellular glycoprotein known to regulate cell-matrix interactions and modulate diverse signaling pathways implicated in angiogenesis, inflammation, and tumorigenesis [32–34]. Although its role function appears to be context-dependent across cancer types [35,36], our findings indicate a tumor-suppressive function in EC. Specifically, we observed a marked downregulation of THBS1 expression in EC cell lines compared with normal ESCs, suggesting a potential loss of tumor-suppressive signaling. Functional assays further demonstrated that forced overexpression of THBS1 in EC cell lines led to reduced cell sur-

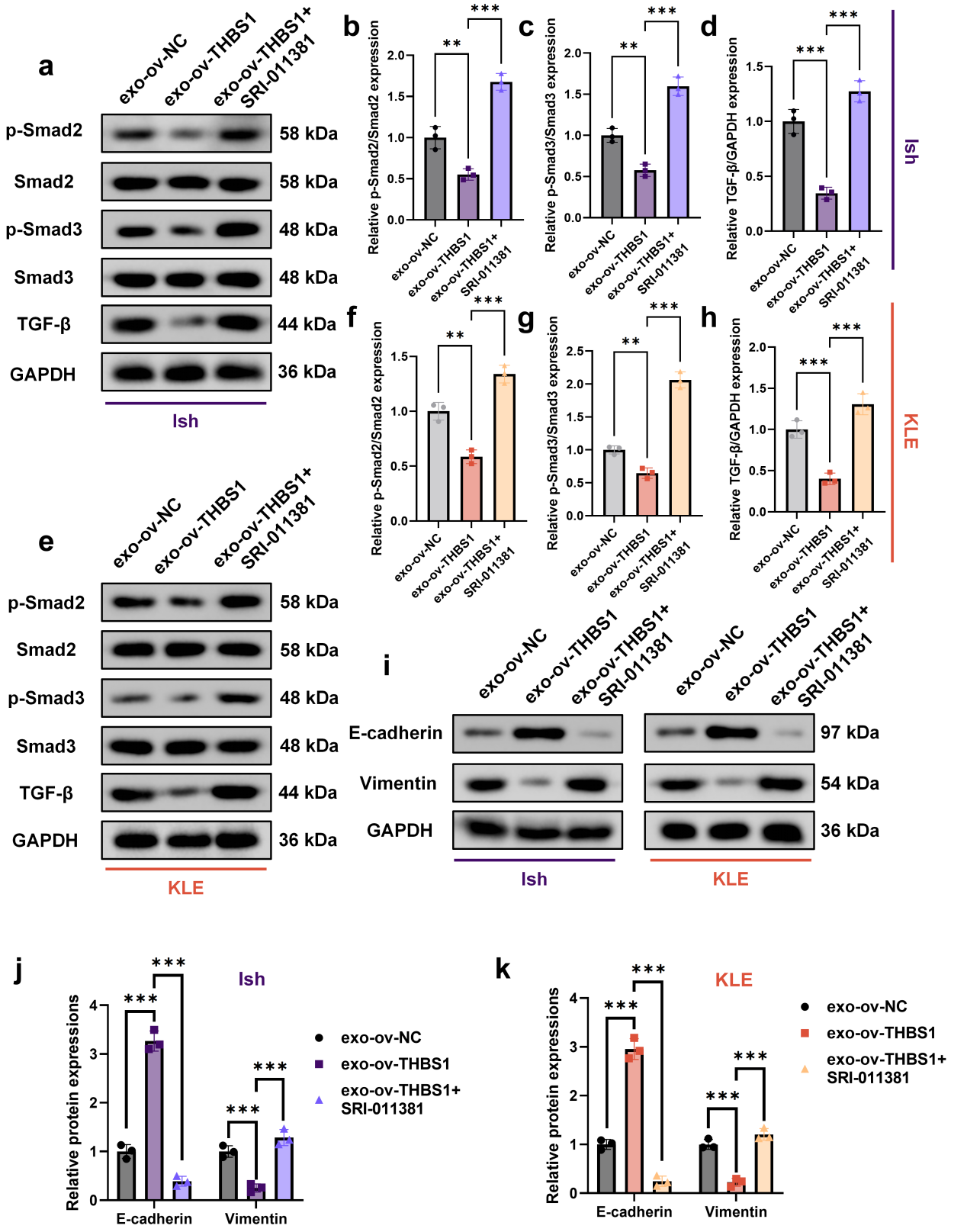

Fig. 6. THBS1-overexpressing HEK293-derived exosomes inhibit TGF-β/Smad signaling and EMT in endometrial cancer cells, which is reversed by the TGF-β activator SRI-011381. (**a**–**d**) Western blot and quantitative analysis of p-Smad2, Smad2, p-Smad3, Smad3, and TGF-β expression in Ish cells treated with HEK293-derived exosomes or exosomes in combination with SRI-011381. (**e**–**h**) Western blot and quantitative analysis of the same signaling proteins in KLE cells under the same treatment conditions. (**i**–**k**) Western blot analysis and quantification of EMT-related markers (E-cadherin, and Vimentin) in Ish and KLE cells treated with HEK293-derived exosomes or exosomes in combination with SRI-011381. $^{**}p < 0.01$, $^{***}p < 0.001$.

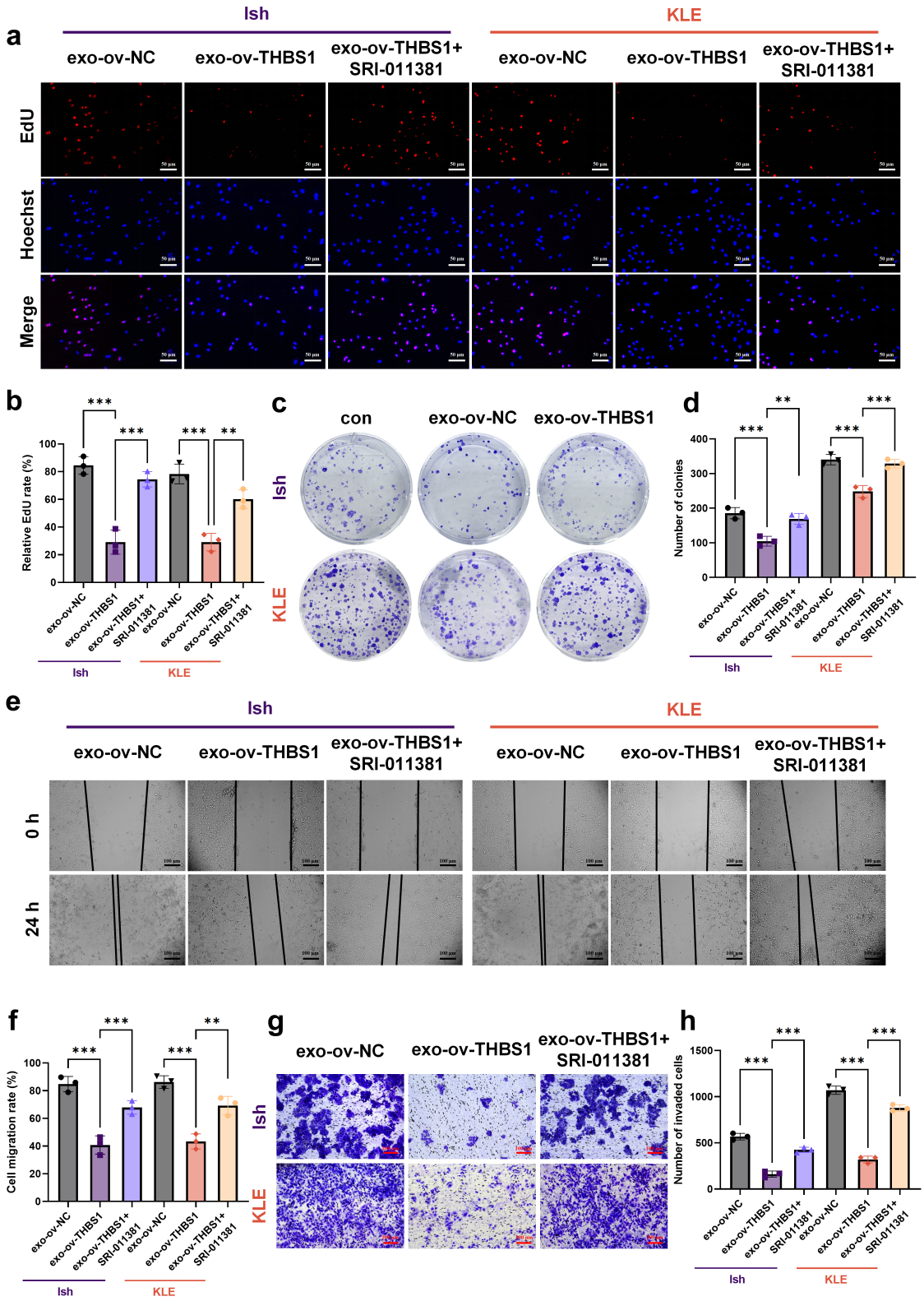

Fig. 7. SRI-011381 reverses the inhibitory effects of THBS1-overexpressing HEK293-derived exosomes on the proliferation, migration, and invasion of endometrial cancer cells. (**a**, **b**) EdU assays evaluating the proliferative capacity of Ish and KLE cells treated with HEK293-derived exosomes alone or in combination with the TGF-β pathway activator SRI-011381 (Scale bar: 50 μm). (**c**, **d**) Colony formation assays assessing the proliferation of Ish and KLE cells under the same treatment conditions. (**e**, **f**) Wound closure assays measuring the migratory ability of Ish and KLE cells following exosome and SRI-011381 treatment (Scale bar: 100 μm). (**g**, **h**) Transwell invasion assays evaluating the invasive capacity of Ish and KLE cells under the indicated treatments (Scale bar: 100 μm). $^{**}p < 0.01$, $^{***}p < 0.001$.

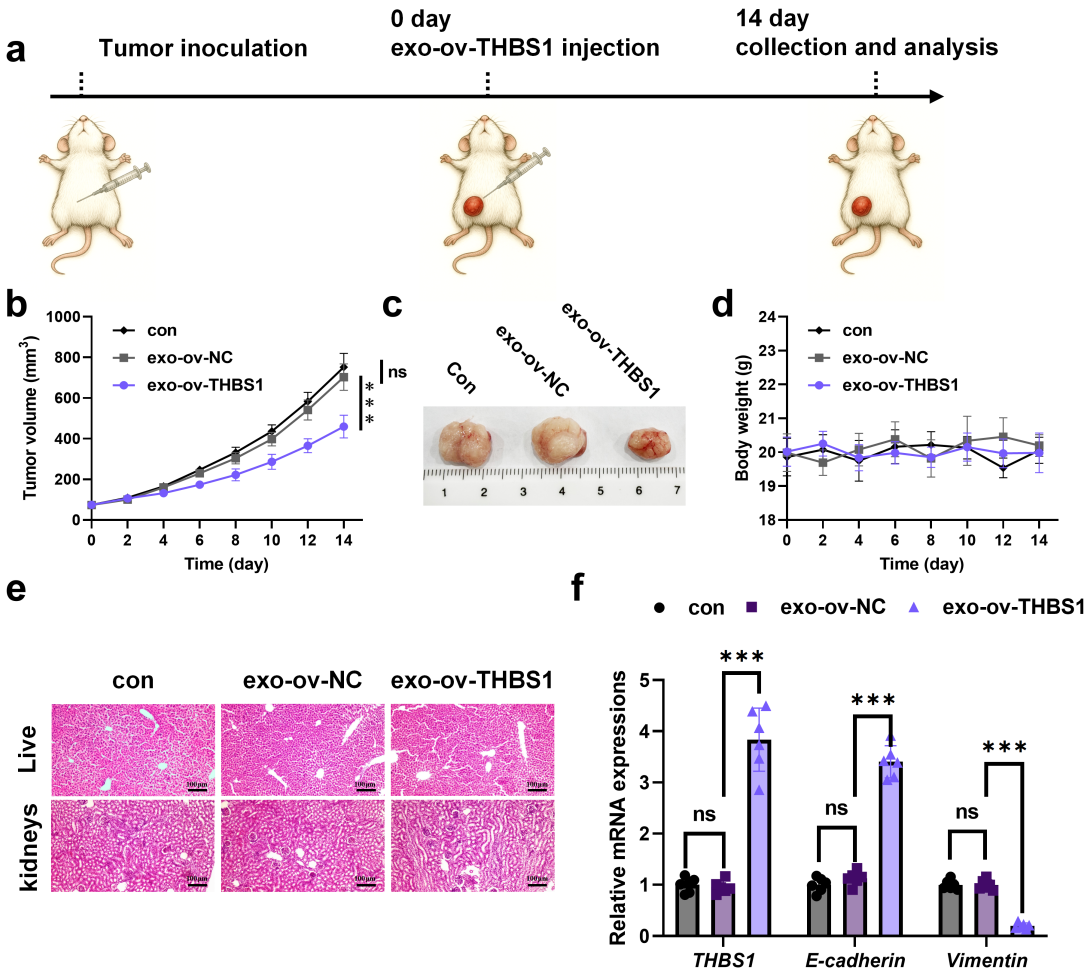

Fig. 8. Effects of HEK293-derived exosomes on tumor growth and EMT marker expression *in vivo*. (**a**) Overview illustration depicting the design of the animal study (created with Microsoft PowerPoint). (**b**) Growth trends of tumors in mice receiving exosome treatments. (**c**) Subcutaneous tumors collected from each experimental group are shown in representative photographs. (**d**) Body weight changes in mice during treatment. (**e**) H&E staining of major organs (liver, and kidney) from treated mice for the assessment of systemic toxicity (Scale bar: 100 μm). (**f**) RT-qPCR analysis of *THBS1*, *E-cadherin*, and *vimentin* expression in tumor tissues. ns, not significant $p > 0.05$, ***$p < 0.001$.

vival, proliferative capacity, and ability to form colonies, alongside notable reductions in migratory and invasive behaviors.

In recent years, exosome-based therapeutic strategies have attracted growing interest because of their ability to mediate intercellular communication and deliver bioactive molecules with high specificity and minimal systemic toxicity. In the present study, exosomes were successfully isolated from HEK293 cells stably overexpressing *THBS1*, and their enrichment with THBS1 protein was confirmed. These engineered exosomes displayed typical cup-shaped morphology under TEM and expressed canonical exosomal markers, including CD9, CD63, CD81, and TSG101. Functionally, treatment with THBS1-enriched exosomes markedly inhibited the proliferation, motility, and invasive capacity of EC cells, closely recapitulating the phenotypic effects of direct *THBS1* overexpression, thereby highlighting their therapeutic potential.

Within the canonical TGF-β/Smad signaling pathway, ligand binding to TGF-β receptors I and II (TβRI and TβRII) activates a signaling cascade that culminates in the phosphorylation, of Smad2 and Smad3 [37]. These phosphorylated Smads then associate with Smad4 to form a transcriptionally active complex that translocates into the nucleus to regulate gene expression programs involved in EMT and tumor progression. Our findings demonstrate that treatment with THBS1-enriched exosomes significantly reduced TGF-β protein expression in EC cells, along with marked reductions in phosphorylated Smad2 and Smad3 levels. This inhibition of TGF-β/Smad signaling was accompanied by upregulation of the epithelial marker E-cadherin and downregulation of the mesenchymal marker vimentin, indicative of EMT suppression. Notably, co-treatment with the TGF-β agonist SRI-011381 reversed

these effects, restoring Smad phosphorylation and EMT marker expression. These results strongly support that the anti-proliferative and anti-invasive effects of THBS1-enriched exosomes are mechanistically dependent on the inhibition of the TGF-β/Smad signaling axis.

To evaluate the translational potential of THBS1-enriched exosomes as a therapeutic strategy, we employed a subcutaneous xenograft mouse model of EC. Systemic administration of THBS1-exosomes via tail vein injection significantly inhibited tumor growth compared to controls. Importantly, no signs of overt systemic toxicity were observed, as indicated by stable body weight and the absence of histopathological abnormalities in major organs such as the liver and kidney. In line with the *in vitro* results, tumors from the THBS1-exosome-treated group showed upregulation of E-cadherin and downregulation of vimentin, supporting the conclusion that THBS1-exosomes suppress tumor progression at least in part through inhibition of EMT *in vivo*. Although IVIS or other real-time tracking techniques were not available in our current facility, the robust antitumor effects observed in the xenograft model strongly suggest that the therapeutic efficacy of the administered exosomes is primarily attributable to their THBS1 enrichment, rather than selective tumor-targeting capabilities. This notion is further supported by the consistent molecular and phenotypic effects of THBS1-overexpressing exosomes observed across both *in vitro* and *in vivo* experimental systems. However, to fully elucidate the biodistribution, tumor-homing potential, and pharmacokinetics of these exosomes, future investigations incorporating *in vivo* imaging and tracking methodologies are warranted. Such studies will be crucial for optimizing targeted delivery strategies and maximizing therapeutic efficacy in clinical settings.

Moreover, the current *in vivo* validation was restricted to a single EC cell line (Ish). While the observed therapeutic effects are encouraging, inclusion of additional cell lines, such as KLE, would enhance the generalizability and translational relevance of our findings by accounting for the molecular heterogeneity of EC. Owing to ethical considerations and resource limitations, the implementation of additional animal cohorts was not feasible within the scope of this study. We acknowledge this as a limitation and propose that future investigations incorporate diverse *in vivo* models to better capture the biological variability and differential responses associated with distinct EC subtypes.

To the best of our knowledge, this study is among the first to employ exosome-based delivery of THBS1 as a strategy to suppress EC malignancy. Engineered exosomes derived from HEK293 cells overexpressing *THBS1* effectively recapitulated the phenotypic effects of direct gene overexpression, markedly inhibiting EC cell proliferation, migration, and invasion. These findings not only reinforce the tumor-suppressive role of *THBS1* but also highlight the therapeutic potential of exosome-mediated protein delivery. This approach offers a biocompatible, low-immunogenic, and potentially tumor-targetable alternative to conventional drug modalities, underscoring its promise as a novel intervention strategy for EC.

Conclusions

THBS1 is downregulated in EC tissues, and its reintroduction markedly suppresses tumor cell proliferation, motility, and invasiveness. Exosomes derived from THBS1-overexpressing cells corroborate these antitumor effects, primarily through the inhibition of the TGF-β/Smad signaling pathway and reversal of EMT. These findings position THBS1—especially when delivered by exosomes—as a compelling and innovative therapeutic candidate for the treatment of EC.

List of Abbreviations

EC, Endometrial cancer; THBS1, Thrombospondin-1; ECM, extracellular matrix; GO, Gene Ontology; KEGG, Kyoto Encyclopedia of Genes and Genomes; TGF-β, transforming growth factor-β; TEM, transmission electron microscopy; NTA, nanoparticle tracking analysis; CCK-8, Cell Counting Kit-8; EMT, epithelial-mesenchymal transition; DEGs, differentially expressed genes; TCGA-UCEC, The Cancer Genome Atlas Uterine Corpus Endometrial Carcinoma; WGCNA, weighted gene co-expression network analysis; TOM, topological overlap matrix; PPI, protein-protein interaction; ESCs, human endometrial stromal cells; DMEM/F12, Dulbecco's modified Eagle's medium/nutrient mixture F-12; FBS, fetal bovine serum; HEK293, Human embryonic kidney 293 cells; Ish, Ishikawa; STR, short tandem repeat; MOI, multiplicity of infection; qRT-PCR, Quantitative Real-Time PCR; PVDF, polyvinylidene fluoride; ECL, enhanced chemiluminescence; PBS, phosphate-buffered saline; L, length; W, width; H&E, hematoxylin and eosin; SD, standard deviation; ANOVA, analysis of variance; p-Smad2, phosphorylated Smad2; p-Smad3, phosphorylated Smad3.

Availability of Data and Materials

The datasets used and analyzed during the current study are available from the corresponding author on reasonable request.

Author Contributions

SYZ and MS contributed to the conceptualization and design of this work. SYZ and WXL contributed to the methodology and formal analysis. CW, YZ, and MS contributed to data acquisition and curation. WPH contributed to formal analysis and visualization. MS contributed to the interpretation of data and critically revised the work for important intellectual content. SYZ and WXL drafted the manuscript. All authors read and approved the final manuscript. All authors agree to be accountable for all aspects of the work in ensuring that questions related to the

accuracy or integrity of any part of the work are appropriately investigated and resolved.

Ethics Approval and Consent to Participate

Animal experiments were conducted in accordance with institutional guidelines and approved by the Animal Ethics Committee of South Zhejiang Institute of Radiation Medicine and Nuclear Technology Applications (ZFY20250110).

Acknowledgments

Not applicable.

Funding

Not applicable.

Conflict of Interest

The authors declare no conflict of interest.

References

[1] Corr BR, Erickson BK, Barber EL, Fisher CM, Slomovitz B. Advances in the management of endometrial cancer. BMJ (Clinical research ed.). 2025; 388: e080978. https://doi.org/10.1136/bmj-2024-080978.

[2] Latif NA, Haggerty A, Jean S, Lin L, Ko E. Adjuvant therapy in early-stage endometrial cancer: A systematic review of the evidence, guidelines, and clinical practice in the U.S. The oncologist. 2014; 19: 645–653. https://doi.org/10.1634/theoncologist.2013-0475.

[3] Wu M, Yang YN, Huang YH, Cai J, He XQ, Wang ZH. Adjuvant chemotherapy versus radiotherapy in high-risk, early-stage endometrioid endometrial carcinoma. Current medical science. 2022; 42: 185–191. https://doi.org/10.1007/s11596-021-2437-8.

[4] How JA, Jazaeri AA, Westin SN, Lawson BC, Klopp AH, Soliman PT, *et al*. Translating biological insights into improved management of endometrial cancer. Nature reviews. Clinical oncology. 2024; 21: 781–800. https://doi.org/10.1038/s41571-024-00934-7.

[5] Yang FF, Zhao TT, Milaneh S, Zhang C, Xiang DJ, Wang WL. Small molecule targeted therapies for endometrial cancer: progress, challenges, and opportunities. RSC medicinal chemistry. 2024; 15: 1828–1848. https://doi.org/10.1039/d4md00089g.

[6] Kumar MA, Baba SK, Sadida HQ, Marzooqi SA, Jerobin J, Altemani FH, *et al*. Extracellular vesicles as tools and targets in therapy for diseases. Signal transduction and targeted therapy. 2024; 9: 27. https://doi.org/10.1038/s41392-024-01735-1.

[7] Bhavsar D, Raguraman R, Kim D, Ren X, Munshi A, Moore K, *et al*. Exosomes in diagnostic and therapeutic applications of ovarian cancer. Journal of ovarian research. 2024; 17: 113. https://doi.org/10.1186/s13048-024-01417-0.

[8] Maqsood Q, Sumrin A, Saleem Y, Wajid A, Mahnoor M. Exosomes in cancer: Diagnostic and therapeutic applications. Clinical Medicine Insights. Oncology. 2024; 18: 11795549231215966. https://doi.org/10.1177/11795549231215966.

[9] Théry C, Witwer KW, Aikawa E, Alcaraz MJ, Anderson JD, Andriantsitohaina R, *et al*. Minimal information for studies of extracellular vesicles 2018 (MISEV2018): A position statement of the international society for extracellular vesicles and update of the MISEV2014 guidelines. Journal of extracellular vesicles. 2018; 7: 1535750. https://doi.org/10.1080/20013078.2018.1535750.

[10] Hushmandi K, Saadat SH, Raei M, Aref AR, Reiter RJ, Nabavi N, *et al*. The science of exosomes: Understanding their formation, capture, and role in cellular communication. Pathology, research and practice. 2024; 259: 155388. https://doi.org/10.1016/j.prp.2024.155388.

[11] Feng Y, Guo K, Jiang J, Lin S. Mesenchymal stem cell-derived exosomes as delivery vehicles for non-coding RNAs in lung diseases. Biomedicine & pharmacotherapy = Biomedecine & pharmacotherapie. 2024; 170: 116008. https://doi.org/10.1016/j.biopha.2023.116008.

[12] Cao L, Ouyang H. Intercellular crosstalk between cancer cells and cancer-associated fibroblasts via exosomes in gastrointestinal tumors. Frontiers in oncology. 2024; 14: 1374742. https://doi.org/10.3389/fonc.2024.1374742.

[13] Chen M, Cao C, Ma J. Tumor-related exosomal circ_0001715 promotes lung adenocarcinoma cell proliferation and metastasis via enhancing M2 macrophage polarization by regulating triggering receptor expressed on myeloid cells-2. Thoracic cancer. 2024; 15: 227–238. https://doi.org/10.1111/1759-7714.15182.

[14] Sahoo RK, Tripathi SK, Biswal S, Panda M, Mathapati SS, Biswal BK. Transforming native exosomes to engineered drug vehicles: A smart solution to modern cancer theranostics. Biotechnology journal. 2024; 19: e2300370. https://doi.org/10.1002/biot.202300370.

[15] Marjani AA, Nader ND, Aghanejad A. Exosomes as targeted diagnostic biomarkers: Recent studies and trends. Life sciences. 2024; 354: 122985. https://doi.org/10.1016/j.lfs.2024.122985.

[16] Xiao Q, Tan M, Yan G, Peng L. Revolutionizing lung cancer treatment: Harnessing exosomes as early diagnostic biomarkers, therapeutics and nano-delivery platforms. Journal of nanobiotechnology. 2025; 23: 232. https://doi.org/10.1186/s12951-025-03306-0.

[17] Cao J, Lv G, Wei F. Engineering exosomes to reshape the immune microenvironment in breast cancer: Molecular insights and therapeutic opportunities. Clinical and translational medicine. 2024; 14: e1645. https://doi.org/10.1002/ctm2.1645.

[18] Bahadorani M, Nasiri M, Dellinger K, Aravamudhan S, Zadegan R. Engineering exosomes for therapeutic applications: Decoding biogenesis, content modification, and cargo loading strategies. International journal of nanomedicine. 2024; 19: 7137–7164. https://doi.org/10.2147/ijn.S464249.

[19] Jung I, Shin S, Baek MC, Yea K. Modification of immune cell-derived exosomes for enhanced cancer immunotherapy: Current advances and therapeutic applications. Experimental & molecular medicine. 2024; 56: 19–31. https://doi.org/10.1038/s12276-023-01132-8.

[20] Tang X, Bi X, Yang A, Wang Q, Yang Y. GGTLC1 knockdown inhibits the progression of endometrial cancer by regulating the TGF-β/Smad signaling pathway. Heliyon. 2024; 10: e31973. https://doi.org/10.1016/j.heliyon.2024.e31973.

[21] Konno T, Kohno T, Kikuchi S, Kura A, Saito K, Okada T, *et al*. The interplay between the epithelial permeability barrier, cell migration and mitochondrial metabolism of growth factors and their inhibitors in a human endometrial carcinoma cell line. Tissue Barriers. 2024; 12: 2304443. https://doi.org/10.1080/21688370.2024.2304443.

[22] Zhang YE, Stuelten CH. Alternative splicing in EMT and TGF-β signaling during cancer progression. Seminars in cancer biology. 2024; 101: 1–11. https://doi.org/10.1016/j.semcancer.2024.04.001.

[23] Wang X, Xue X, Pang M, Yu L, Qian J, Li X, *et al*. Epithelial-mesenchymal plasticity in cancer: Signaling pathways and therapeutic targets. MedComm. 2024; 5: e659. https://doi.org/10.1002/mco2.659.

[24] Garg P, Pareek S, Kulkarni P, Horne D, Salgia R, Singhal SS. Exploring the potential of TGFβ as a diagnostic marker and therapeutic target against cancer. Biochemical pharmacology. 2025; 231: 116646. https://doi.org/10.1016/j.bcp.2024.116646.

[25] Su W, Hu S, Zhou L, Bi H, Li Z. FOXP2 inhibits the aggressiveness of lung cancer cells by blocking TGFβ signaling. Oncology letters. 2024; 27: 227. https://doi.org/10.3892/ol.2024.14361.

[26] Festing MF. On determining sample size in experiments involving

laboratory animals. Laboratory animals. 2018; 52: 341–350. https://doi.org/10.1177/0023677217738268.

[27] Niebora J, Woźniak S, Domagała D, Data K, Farzaneh M, Zehtabi M, *et al*. The role of ncRNAs and exosomes in the development and progression of endometrial cancer. Frontiers in oncology. 2024; 14: 1418005. https://doi.org/10.3389/fonc.2024.1418005.

[28] Bian Y, Chang X, Hu X, Li B, Song Y, Hu Z, *et al*. Exosomal CTHRC1 from cancer-associated fibroblasts facilitates endometrial cancer progression via ITGB3/FAK signaling pathway. Heliyon. 2024; 10: e35727. https://doi.org/10.1016/j.heliyon.2024.e35727.

[29] Ebrahimi N, Manavi MS, Faghihkhorasani F, Fakhr SS, Baei FJ, Khorasani FF, *et al*. Harnessing function of EMT in cancer drug resistance: A metastasis regulator determines chemotherapy response. Cancer metastasis reviews. 2024; 43: 457–479. https://doi.org/10.1007/s10555-023-10162-7.

[30] Gopinatha Pillai MS, Shaw P, Dey Bhowmik A, Bhattacharya R, Rao G, Dhar Dwivedi SK. Uterine carcinosarcoma: Unraveling the role of epithelial-to-mesenchymal transition in progression and therapeutic potential. FASEB journal : official publication of the Federation of American Societies for Experimental Biology. 2024; 38: e70132. https://doi.org/10.1096/fj.202401991R.

[31] Himani, Kaur C, Kumar R, Mishra R, Singh G. Targeting TGF-β: A promising strategy for cancer therapy. Medical oncology (Northwood, London, England). 2025; 42: 142. https://doi.org/10.1007/s12032-025-02667-8.

[32] Pervaiz N, Kathuria I, Aithabathula RV, Singla B. Matricellular proteins in atherosclerosis development. Matrix biology : journal of the International Society for Matrix Biology. 2023; 120: 1–23. https://doi.org/10.1016/j.matbio.2023.04.003.

[33] Kaur S, Bronson SM, Pal-Nath D, Miller TW, Soto-Pantoja DR, Roberts DD. Functions of Thrombospondin-1 in the tumor microenvironment. International journal of molecular sciences. 2021; 22: 4570. https://doi.org/10.3390/ijms22094570.

[34] Li S, Sampson C, Liu C, Piao HL, Liu HX. Integrin signaling in cancer: Bidirectional mechanisms and therapeutic opportunities. Cell communication and signaling: CCS. 2023; 21: 266. https://doi.org/10.1186/s12964-023-01264-4.

[35] Mu Y, Wallenius A, Zang G, Zhu S, Rudolfsson S, Aripaka K, *et al*. The TβRI promotes migration and metastasis through thrombospondin 1 and ITGAV in prostate cancer cells. Oncogene. 2024; 43: 3321–3334. https://doi.org/10.1038/s41388-024-03165-3.

[36] Zeng Z, Lin C, Zhang MC, Kossinna P, Wang P, Cao D, *et al*. Enterolactone and trabectedin suppress epithelial ovarian cancer synergistically via upregulating THBS1. Phytotherapy research: PTR. 2023; 37: 4722–4739. https://doi.org/10.1002/ptr.7942.

[37] Klenk HP, Clayton RA, Tomb JF, White O, Nelson KE, Ketchum KA, *et al*. The complete genome sequence of the hyperthermophilic, sulphate-reducing archaeon Archaeoglobus fulgidus. Nature. 1997; 390: 364–370. https://doi.org/10.1038/37052.

Editor's note: The Scientific Editor responsible for this paper was Bo Lei and Martin Stoddart.

Received: 21st June 2025; **Accepted**: 2nd March 2026; **Published**: 30th April 2026